The State of Charge Balancing Techniques For Electrical Vehicle Charging Stations With Cascaded H-Bridge Multilevel Converters

Amirhossein Moeini, and Shuo Wang
Power Electronics and Electric Power Research Laboratory, Department of Electrical and Computer Engineering,
University of Florida
Gainesville, Florida, USA
ahm1367@ufl.edu, shuowang@ieee.org

***Abstract*— In this paper, two state-of-charge (SOC) balancing techniques are proposed for an electrical vehicle charging station which is based on a grid-tied cascaded H-bridge (CHB) multilevel converter. The first proposed technique uses the redundant states of the CHB converter to generate different AC voltages to balance the SOCs of the CHB cells. For the first proposed technique, the active power injected to the CHB converter is calculated and the optimal switching state that can regulate the SOCs of batteries is designed before switching transitions. In the second proposed technique, the information of AC input current is employed to design the switching states at each quarter of the period. As shown in this paper, the two proposed techniques can regulate the SOCs of the multilevel converter much faster than two conventional techniques in literature without increasing cost or complexity of the converter. This can increase the battery charging speed on the grid-tied converter. The experiments are conducted on a 7-level CHB converter to validate the two proposed techniques.**

***Index Terms*—State of charge balancing, cascaded H-bridge, electrical vehicle charging station, selective harmonic current mitigation.**

I. INTRODUCTION

The battery energy storage system (BESS) can be used for different applications such as electrical vehicle charging stations (EVCS), renewable energies, and smart grids [1][2][3]. The grid-tied converters can be connected to the BESS to control the active and reactive power of power grid, transfer active power to the EVCS, and meet the requirements of power quality standards [3][4][5].

The grid-tied cascaded H-bridge converter has advantages over other types of grid-tied converters because of its modular structure and redundant states to generate different voltage levels [6]. Different modulation techniques such as phase shift-pulse width modulation (PS-PWM) [4], space vector modulation (SVM) [7], selective harmonic elimination-pulse width modulation (SHE-PWM) [6], selective harmonic mitigation-PWM (SHM-PWM) [8] and selective harmonic current mitigation-PWM (SHCM-PWM) [4-5] [9] were used in literature for the CHB converters. Among all of these, the SHCM-PWM can meet the current harmonic requirements of power quality standards, increase the efficiency of the converter, and reduce the size of passive filters [4].

This work was supported by National Science Foundation under Award Number 1540118.

One of the main challenges of the grid-tied CHB converter in EVCSs is the balancing speed of the state of charges (SOCs). This is so important due to increasing the charging speed of the batteries. Different techniques in literature have been proposed to balance the SOCs of batteries that are connected to the CHB converter [10-11]. In [10], the SOC balancing can be achieved by checking the power factor and the SOCs of batteries in each half-period. Then, the best switching states are selected among all of the available switching states at each half-period. Even though this technique can balance the SOCs of batteries for different active and reactive power, the balancing speed with this technique is slow due to non-optimal selection of switching states at all periods, when the reactive power is injected or absorbed from the power grid.

In [11], a swapping first on first off SOC balancing technique is proposed for the CHB converter so that the switching states in each half-period are selected to balance the SOCs of batteries. Even though this technique can balance the SOCs of batteries faster than [10] due to swapping the switching states of the CHB converter in each half-period, the balancing speed of this technique still is slow due to using non-optimal switching states in several of the half periods (only in one half-period out of three half-periods the applied switching states in [11] is optimal).

In [6] and [12], a capacitor voltage balancing technique is proposed for the multilevel CHB converter to balance the DC link capacitor voltages. In the proposed technique by measuring the terminal voltages of DC links and the instantaneous active power which is applied to the CHB converter before each switching transition, the best switching state is selected among the available redundant states of the multilevel CHB converter. As a result, this technique can balance and regulate the DC link capacitor voltages much faster and more efficient than other techniques in literature. However, this technique has not been employed on the EVCSs to balance the SOCs of batteries.

In this paper, two new techniques are proposed to balance the SOCs of batteries in the CHB converter. In the first proposed technique, the active power, which flows from the power grid to the cells of the CHB converter, is measured

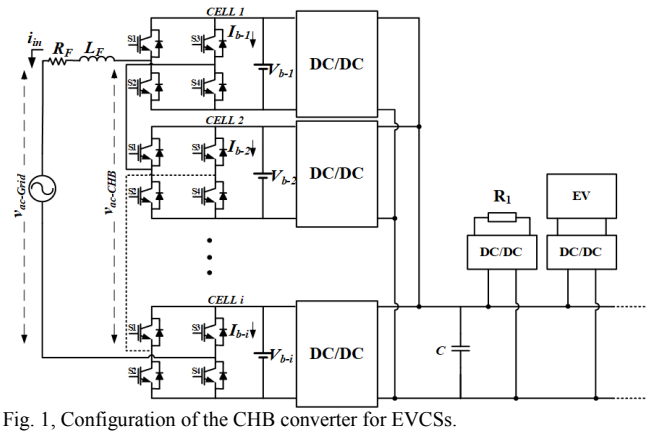

Fig. 1, Configuration of the CHB converter for EVCSs.

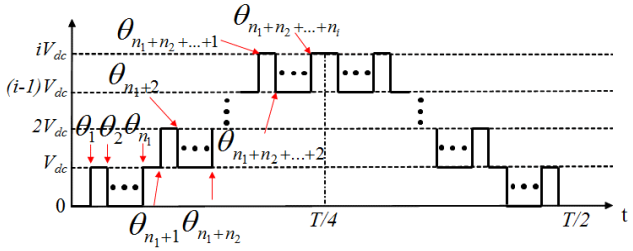

Fig. 2, Predefined waveform of an *i*-cell CHB converter.

before each switching transitions. Then based on the available redundant states of the CHB converter to generate different voltage levels, the best switching states are applied to the next switching transition. Also, in the second SOC balancing technique, the information of AC input current is used to select the best switching states in each quarter-period. The proposed techniques in this paper can balance the SOCs of the CHB converter much faster than the two conventional techniques [10-11] as will be proven, when the CHB converter injects or absorbs reactive power from the power grid.

II. The Grid-Tied Cascaded H-Brige Converter With Selective Harmonic Current Mitigation-PWM

Fig. 1 shows a configuration of an *i*-level CHB converter that is connected to the DC/DC converters to feed the required active power to the DC link capacitor (*C*). The DC/DC converters can provide galvanic isolations for EVCSs. The I_{b-1}, and V_{b-1} are the battery voltage and current for the first cell of the CHB converter, respectively. Because the main goal of this paper is to achieve the fast SOC balancing for the CHB converter, the DC/DC converter stage is not the focus of this paper. In Fig. 1, the KVL equation of the AC side of CHB converter can be written as,

$$v_{ac-Grid}(t) + R_F i_{in}(t) + L_F \frac{di_{in}(t)}{dt} = v_{ac-CHB}(t) \quad (1)$$

where L_F, and R_F are the coupling inductance and its parasitic resistance, respectively. The $v_{ac\text{-}CHB}$(t), $v_{ac\text{-}Grid}$(t), and i_{in}(t) are the fundamental AC voltage of the CHB, the fundamental AC grid voltage and the AC input current of the CHB converter, respectively. The SHCM-PWM [5] is used as the modulation technique in this paper. The objective function set of the SHCM-PWM technique is shown in (2) which is used for the predefined waveform in Fig. 2. To obtain (2), the Fourier series of the predefined waveform in Fig. 2 are derived for the fundamental (the first term in (2)) and higher order of harmonic components (the 3rd term in (2)) as discussed in [5]. The second term in (2) meets the total demand distortion (TDD).

$$\begin{cases} M_a = \cos\theta_1 - \cos\theta_2 + \cos\theta_3 ... + \cos\theta_k \\ \sqrt{\left(\frac{I_{in-3}}{I_1}\right)^2 + \left(\frac{I_{in-5}}{I_1}\right)^2 + ... + \left(\frac{I_{in-h}}{I_1}\right)^2 + ...} \le C_{TDD} \\ \frac{|V_{ac-Grid-h}| + |V_{ac-CHB-h}|}{|\omega h L_F I_L|} \le C_h, h = 3,5,7,... \end{cases} \quad (2)$$

where M_a is the modulation index of the CHB converter. θ_1, θ_2,…, θ_k are the switching angles of the CHB converter with the SHCM-PWM. I_{in-3}, I_{in-5},…, I_{in-h} are the current harmonic magnitudes for 3rd, 5th, …, h^{th} harmonic orders, respectively. I_L is the maximum demand load current based on the IEEE 519 2014 [13] standard. The C_h, and C_{TDD} are the current harmonic and TDD limits based on IEEE 519 2014 standard in Table I.

TABLE I. HARMONIC LIMITS OF IEEE 519 2014 STANDARD [13].

$I_{sc}/I_L \le 20$	$h<11$	$11 \le h<17$	$17 \le h<23$	$23 \le h<35$	$35 \le h \le 50$	C_{TDD}
$C_{h\ \&\ TDD}$	4%	2%	1.5%	0.6%	0.3%	5%

The details of how to extract and solve the equation set in (2) is fully discussed in [5]. The main goal of this paper is to balance the SOCs of batteries in the CHB converter by using the SHCM-PWM technique.

III. The Proposed Techniques For The SOC Balancing Of The CHB Converter

A. Conventional SOC balancing techniques

The main idea of balancing the SOCs of batteries in an *i*-cell CHB converter is to inject more active power to the cell which has lower SOC and inject less active power to the cell which has higher SOC [10-11]. Two techniques are proposed in the literature [10-11] to reach this goal.

Fig. 3 shows the SOC balancing techniques in [10], and [11] when the SOCs of cells are $SOC_3<SOC_2<SOC_1$. In [10] as shown in Fig. 3(a), at each half-period, the power quality of the CHB converter is checked. Then, the SOCs are sorted. Furthermore, during charging the cell which has lower SOC, turns on more than the rest of the cells by choosing the longer staircase waveform in each half-period as shown in Fig. 3 (a). Contrarily, the cell which has higher SOC, is turned on less than the other cells by choosing the shorter staircase waveform. As a result, when the SOCs are $SOC_3<SOC_2<SOC_1$, the third, second and first cells are sequentially turned on in the first quarter of period and the first, second and third cells are sequentially turned off in the second quarter of period. Although the proposed technique can optimally balance SOCs for the case that AC input current is in phase with the AC CHB voltage, it cannot balance the SOCs of batteries as fast as possible when the reactive power is injected or absorbed from the power grid during charging of the CHB converter.

In the second conventional technique in [11], the swapping first on and first off technique is proposed to balance the SOCs of batteries. In this technique, the cells' SOC and the power factor of the CHB converter are measured at each half-period similar to [10]. Then, in the first quarter of period, the cells are sequentially turned on similar to [10]. For the second quarter of period, a technique is used to swap all of the available

switching states between the cells of the CHB as shown in Fig. 3 (b). For example, when the SOCs are $SOC_3<SOC_2<SOC_1$ and active power is injected to the CHB converter, the third, second and first cells are turned on for the first, second and third voltage levels in all of the half-periods, respectively. Also, they are sequentially turned off at the first, second and third voltage levels as shown in Fig. 3(b) for the first half-period and for the next two half-periods, the swapping technique is used to employ all of the different voltage levels of the CHB to different cells of the CHB. This technique can charge cells more efficiently than the first technique, because at least in one of the three half-period in Fig. 3(b), the injected power to the cells of the CHB converter is optimal. However, this technique cannot apply optimal switching states to the CHB converter for all of the half-periods due to using non-optimal switching states for the CHB converter in two half-periods out of three half-periods. The two conventional techniques [10][11] also can be extended for the discharging mode of the CHB converter.

B. The first proposed SOC balancing technique

The CHB converter has the redundant states to generate different voltage levels. In Fig. 4 (a), the first proposed SOC balancing technique is shown. As shown in Table II, for V_{dc}, $2V_{dc}$, $-V_{dc}$, and $-2V_{dc}$, there are redundant states which can be used to balance the SOCs. In the first proposed technique, before each switching transitions both SOCs and the sign of instantaneous active power are checked. As an example, in the switching transition between zero level and first level (V_{dc}); (a) If the sign of instantaneous active power that flows through the cells is positive, then the cell which has the lowest SOC is turned on. (b) If the sign of instantaneous power that flows through the cells is negative, then the cell which has the lowest SOC is turned on. This balancing technique can be done for all levels of the CHB (except the highest voltage level) voltage waveform which have redundant states. Because in the proposed technique, the SOCs are continousely controlled based on instantaneous active power that is injected to the CHB, the proposed technique can balance the SOCs much faster than the two conventional techniques. As an example in Fig. 4 (a), when the SOCs of the CHB converter are $SOC_3<SOC_2<SOC_1$, because the sign of active power is positive in the first quarter of the period, the third, second and first cells are sequentioally turned on. In the second quarter of period as shown in Fig. 4(a), the sequence of switchings are the first, third, and second cells, respectively, due to the changes of sign for the active power at the second quarter-period.

The first proposed technique still does not apply the optimal switching angles to balance the SOCs of cells. As shown in Fig. 4(a), the first cell is turned off in Θ_4, even though the instantaneous active power is negative in most of the rest of the quarter-period. So, using the instantaneous active power to balance the SOCs cannot give the optimal result, when the best switching states are selected before each switching transitions.

C. The second proposed SOC balancing technique

To solve the issue of the first proposed technique, the time instant that the direction of AC current is changed from positive to negative can be used to balance the SOCs of batteries. As shown in the first half-period waveform in Fig. 4(a), in either the first or second quarter-period, the sign of AC current does not change (positive/charging or negative/discharging) and in the other quarter-period, the sign of AC current is changed from positive to negative or negative to positive. For the first quarter-period (the sign of current does not change), the SOCs are sorted and similar to the first and second conventional techniques, the cell which has lower SOC is turned on longer than the other cells during charging or turned on shorter than the other cells during discharging. For the other quarter-period based on the time instant that the current sign is changed, the switching states can be selected. It is important to note that the switching states of the CHB converter during the second quarter-period (the sign of AC current is changed) depend on the obtained switching angles of SHCM-PWM technique for different modulation indices, and the time instant that the AC current sign is changed. So, optimal switching states are functions of modulation indices and the time instant that the sign of AC current is changed. Table III shows an example of optimal switching states of the CHB converter for the second proposed technique when the sign of AC current is changed between Θ_1 and Θ_6 in Fig. 4(b) and the SOCs are $SOC_3<SOC_2<SOC_1$. Table III considers both the charging (ch) and discharging (disch) modes. It is important to note that based on the switching angles of the SHCM-PWM, the optimal switching states of Table III can be changed. Obtaining all of the optimal switching states for different modulation indices can significantly increase the size of algorithm during experiment. So, in this paper, a table similar to Table III is considered for all of the modulation indices. The second proposed technique can reach the fastest SOC balancing technique, if the sign of AC current and the switching angles of different modulation indices are checked and the best switching states are designed before each quarter-period.

Since, the switching states are symmetrical in two half-periods for the first conventional, the first proposed, and the second proposed techniques, they can have high reliability due to not increasing unequally the temperatures of switches of cells. However, the second conventional technique increases unequally the temperatures of switches due to asymmetrical switching transitions in two half-periods as shown in Fig. 3(b).

D. The controller design for the proposed SOC balancing techniques

The proposed SOC balancing techniques need to use closed-loop controller to control both magnitude and phase of the current to the required values. Also, the proposed controller should be able to control the average currents which are passed through the cells. The average current which is applied to the *i*th cell of the CHB converter can be obtained as follow,

$$i_{b-avg-k} = \frac{1}{T}\int_{T} i_{b-k}(t)dt = \frac{1}{T}\int_{T_k} i_{in}(t)dt \qquad (3)$$

where T_k is the duration of time that the *k*th cell is turned on during the period *T*. *T* is the period of fundamental frequency. Moreover, the $i_{b\text{-}avg\text{-}k}$ is the average current of the *k*th cell of the CHB converter. The $i_{in}(t)$ in (3) can have all harmonic orders, however, the fundamental frequency only has huge influence on the average current. So, the following equation instead of (3) can be used for the first cell in Fig. 4 (a),

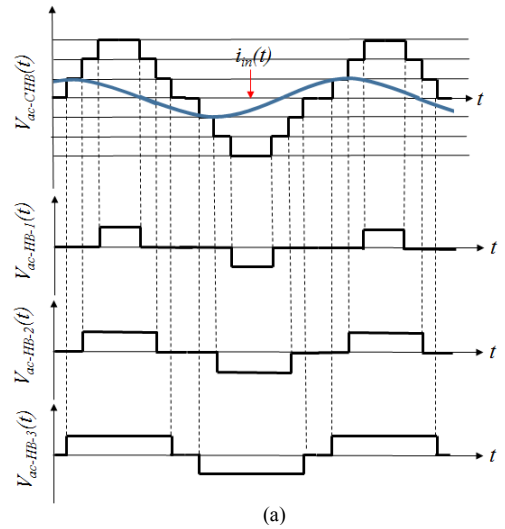

(a)

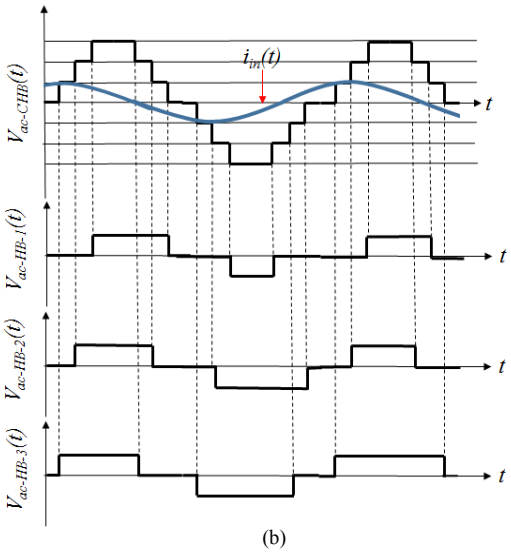

(b)

Fig. 3, Waveforms of generated voltages of the three-cell CHB converter when the SOCs are $SOC_3<SOC_2<SOC_1$, (a) technique in [10], (b) technique in [11].

$$i_{b-avg-1} = \frac{1}{\pi}\int_{\theta_3}^{\theta_4} I_{in}\sin(\theta+\theta_0)d\theta \tag{4}$$

where Θ_0 is the initial phase of the AC input current. The maximum average currents which are applied to all of the cells of the CHB converter can be obtained by the following equation,

$$\sum_{k=1}^{i} i_{b-avg-k} = \sum_{k=1}^{i}(\frac{1}{\pi}\int_{\theta_k} I_{in}\sin(\theta+\theta_0)d\theta) = \tag{5}$$

$$\frac{2I_{in}}{\pi}(\cos(\theta_1+\theta_0)-\cos(\theta_2+\theta_0)+...) = f(I_{in}, M_a, \theta_0)$$

As shown in (5), to control the total average current which is applied to the CHB cells, the current magnitude, the modulation index of the CHB converter, and the initial phase of AC current should be controlled. Also, the SOC of each cell of the CHB can be obtained by the following equation,

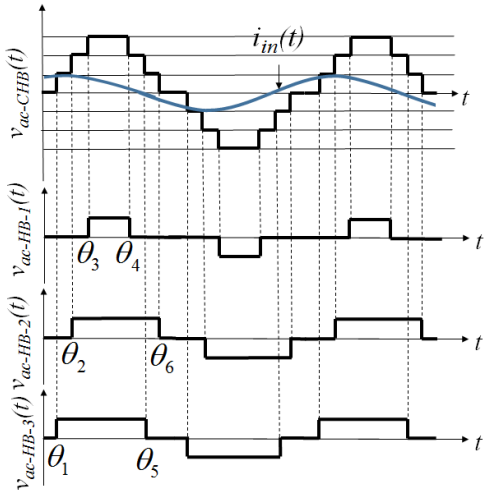

(a)

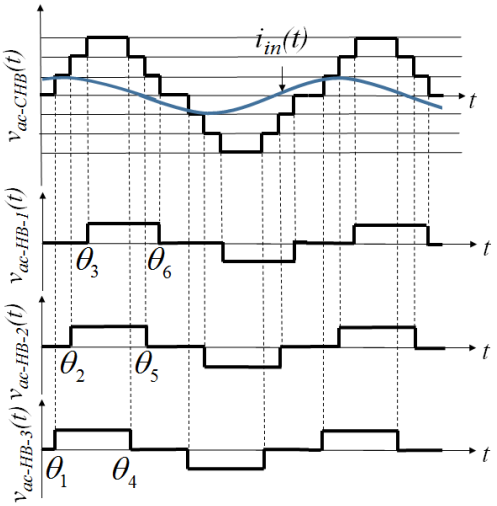

(b)

Fig. 4, Waveforms of the generated voltages of the three-cell CHB converter when the SOCs of cells are $SOC_3<SOC_2<SOC_1$, (a) the first proposed technique, (b) the second proposed technique.

$$SOC_k(t) = SOC_{k0} - \frac{1}{C_b}\int i_{b-k}(t)dt, \tag{6}$$

where C_b is the nominal capacity of the battery in the kth cell of the CHB converter. SOC_{k0} is the initial value of SOC of the kth cell of the CHB converter. The SOC of each cell depends on the average current of the battery. If the SOC of all cells are controlled to the same values, then based on (3) and (6), the following condition should be met by the CHB converter, when the same batteries are used on the cells of the CHB converter.

$$i_{dc-avg-1} = i_{dc-avg-2} = ... = i_{dc-avg-i}, \tag{7}$$

The proposed controller in this paper should be able to control the AC current magnitude and phase for the CHB converter. Also, it should be able to control the modulation index and the phase of the CHB converter based on (5).

Moreover, as shown in (7), when the SOCs are controlled to the same value, it should be able to control the average currents of the cells to the same value. Fig. 5 shows the proposed controller to charge the batteries of the grid-tied CHB converter.

The sum of the average currents of cells of the CHB converter are measured and added together. Then, the mean of these average currents is compared with the reference average current $I_{dc\text{-}avg\text{-}ref}^{*}$. As shown in Fig. 5, the error of them is applied to a PI controller. As shown in (5), to control the average currents of the cells, the AC current magnitude I_{in}, the modulation index M_a, and the initial phase of current θ_0 should be controlled. So, in Fig. 5, the output of the first PI controller in Fig. 5 is the I_{in}^{*}. Then, the measured AC current magnitude I_{in} is compared with the I_{in}^{*}. The error of them is also applied to a second PI controller. The output of the second PI controller determines the modulation index of the CHB converter. This is due to the fact that by controlling the CHB voltage phase and magnitude, the AC input current from the power grid to the CHB converter can be controlled, when the fundamental AC grid voltage magnitude and phase are considered as reference. As a result, another PI controller is used in the proposed controller in Fig. 5 to control the phase difference between the grid voltage and AC input current $\angle v_{ac-Grid} - \angle i_{in}$ (where $\angle i_{in} = \theta_0$).

The designed controller in Fig. 5 has three PI controllers to control all of the three parameters that affect the average currents which are injected to the cells of the CHB converter in (6). The outputs of these three PI controllers determine the modulation index (M_a) and the initial phase of the CHB converter θ_{CHB} as shown in Fig. 5.

The optimization techniques are used in many different applications such as wind powers [14], distributed generations (DGs) [15] and grid-tied converters [16]. In this paper the particle swarm optimization technique is used for the SHCM-PWM technique in the experiments. The LUTs, which store the solutions of modulation indices of SHCM-PWM in (2), select the switching angles and apply them to the SOC balancing unit. Then either of four balancing techniques can be used to balance the SOCs of the CHB converter.

IV. Experimental Results

To validate the performance of the proposed SOC balancing technique in a grid-tied CHB converter, several experimental results are obtained for a 3-cell 7-level CHB converter.

The TMS320F28335 digital signal processor is used in this paper for the proposed SOC balancing technique with the designed controller in Fig. 5. The parameters of a 7-level CHB converter are shown in Table IV. The batteries, which are used in the experiments, are lead acid. As shown in Table IV, 5 batteries are connected in series for each cell of the CHB converter.

In Fig. 6, the hardware prototype, which is used in the experiments, is shown.

In the first experimental result, the time domain waveforms of the CHB converter are shown in steady state condition. As shown in Fig. 7, the current magnitude of the CHB converter is limited to 4.2A and 120 degrees. This curent can discharge the batteries. As shown in Fig. 7(b), the harmonic spectrum of the experimental result meets the current requirements of IEEE 519 standard [13]. Also, the total demand distortion (TDD) can meet the 5% requirements of IEEE 519 2014 [13] standard.

TABLE II, First proposed SOC balancing technique with the redundant states of the CHB converter for V_{dc} $2V_{dc}$, and $3V_{dc}$.

Voltage Level	*SOC states*	*Sign ($P_{avg\text{-}conv}$)*	*Switching states*
V_{dc}	$soc_1 \le soc_2 \le soc_3$	+	$sw_1=1, sw_2=0, sw_3=0,$
V_{dc}	$soc_1 \le soc_2 \le soc_3$	-	$sw_1=0, sw_2=0, sw_3=1,$
V_{dc}	$soc_1 \le soc_3 \le soc_2$	+	$sw_1=1, sw_2=0, sw_3=0,$
V_{dc}	$soc_1 \le soc_3 \le soc_2$	-	$sw_1=0, sw_2=1, sw_3=0,$
V_{dc}	$soc_2 \le soc_1 \le soc_3$	+	$sw_1=0, sw_2=1, sw_3=0,$
V_{dc}	$soc_2 \le soc_1 \le soc_3$	-	$sw_1=0, sw_2=0, sw_3=1,$
V_{dc}	$soc_2 \le soc_1 \le soc_3$	+	$sw_1=0, sw_2=1, sw_3=0,$
V_{dc}	$soc_2 \le soc_1 \le soc_3$	-	$sw_1=0, sw_2=0, sw_3=1,$
V_{dc}	$soc_2 \le soc_3 \le soc_1$	+	$sw_1=0, sw_2=1, sw_3=0,$
V_{dc}	$soc_2 \le soc_3 \le soc_1$	-	$sw_1=1, sw_2=0, sw_3=0,$
V_{dc}	$soc_3 \le soc_1 \le soc_2$	+	$sw_1=0, sw_2=0, sw_3=1,$
V_{dc}	$soc_3 \le soc_1 \le soc_2$	-	$sw_1=0, sw_2=1, sw_3=0,$
$2\ V_{dc}$	$soc_1 \le soc_2 \le soc_3$	+	$sw_1=1, sw_2=1, sw_3=0,$
$2\ V_{dc}$	$soc_1 \le soc_2 \le soc_3$	-	$sw_1=0, sw_2=1, sw_3=1,$
$2\ V_{dc}$	$soc_1 \le soc_3 \le soc_2$	+	$sw_1=1, sw_2=0, sw_3=1,$
$2\ V_{dc}$	$soc_1 \le soc_3 \le soc_2$	-	$sw_1=0, sw_2=1, sw_3=1,$
$2\ V_{dc}$	$soc_2 \le soc_1 \le soc_3$	+	$sw_1=1, sw_2=1, sw_3=0,$
$2\ V_{dc}$	$soc_2 \le soc_1 \le soc_3$	-	$sw_1=1, sw_2=0, sw_3=1,$
$2\ V_{dc}$	$soc_2 \le soc_3 \le soc_1$	+	$sw_1=0, sw_2=1, sw_3=1,$
$2\ V_{dc}$	$soc_2 \le soc_3 \le soc_1$	-	$sw_1=1, sw_2=0, sw_3=1,$
$2\ V_{dc}$	$soc_3 \le soc_1 \le soc_2$	+	$sw_1=1, sw_2=0, sw_3=1,$
$2\ V_{dc}$	$soc_3 \le soc_1 \le soc_2$	-	$sw_1=1, sw_2=1, sw_3=0,$
$2\ V_{dc}$	$soc_3 \le soc_2 \le soc_1$	+	$sw_1=0, sw_2=1, sw_3=1,$
$2\ V_{dc}$	$soc_3 \le soc_2 \le soc_1$	-	$sw_1=1, sw_2=1, sw_3=0,$
$3\ V_{dc}$	--	--	$sw_1=1, sw_2=1, sw_3=1,$

TABLE III, An example of switching angles of the second proposed technique when $SOC_3<SOC_2<SOC_1$ for the quarter-period that the sign of AC current is changed.

The sign of current	First voltage level		Second voltage level		Third voltage level	
	ch	disch	ch	disch	ch	disch
$\Theta_1 < \Theta_0 - \Theta_{CHB} < \Theta_2$	Cell2	Cell2	Cell3	Cell1	Cell1	Cell3
$\Theta_2 < \Theta_0 - \Theta_{CHB} < \Theta_3$	Cell1	Cell3	Cell2	Cell2	Cell3	Cell1
$\Theta_3 < \Theta_0 - \Theta_{CHB} < \pi/2$	Cell1	Cell3	Cell2	Cell2	Cell3	Cell1
$\pi/2 < \Theta_0 - \Theta_{CHB} < \Theta_4$	Cell1	Cell3	Cell2	Cell2	Cell3	Cell1
$\Theta_4 < \Theta_0 - \Theta_{CHB} < \Theta_5$	Cell1	Cell3	Cell2	Cell2	Cell3	Cell1
$\Theta_5 < \Theta_0 - \Theta_{CHB} < \Theta_6$	Cell2	Cell2	Cell3	Cell1	Cell1	Cell3

TABLE IV. Circuit parameters of the proposed techniques during experiment.

Parameter	Symbol	Value
Line frequency	F	60 Hz
Ac grid Voltage (RMS)	$V_{ac\text{-}Grid}$	110 V
Total rated power	S_{total}	1.550 kVA
Maximum Demand Load (RMS)	I_L	14.14 A
Number of H-bridge cells	i	3
Number of switching transitions in half-period	K	18
Highest order of mitigated harmonic	H	49th
Inductance	L_F	0.4845pu
Resistance of inductance	R_F	0.0643pu
Impedance of DC link Capacitor	$1/\omega C$	0.0775pu
Nominal battery voltage	V_n	12V
Nominal battery capacity	C_b	12Ah
Number of batteries in series for each cell	N_b	5

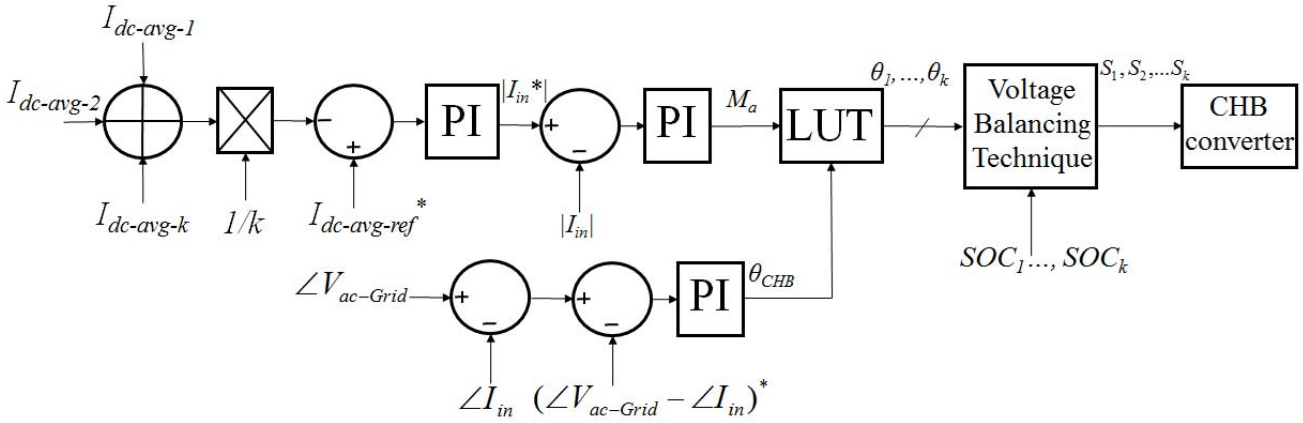

Fig. 5, Control block of the grid-tied CHB converter.

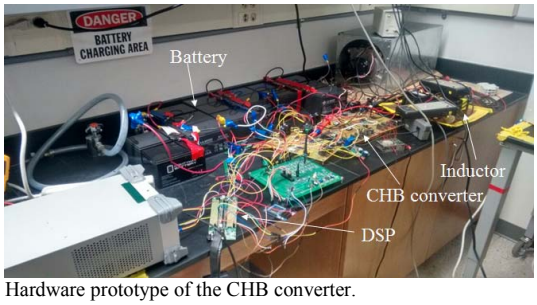

Fig. 6, Hardware prototype of the CHB converter.

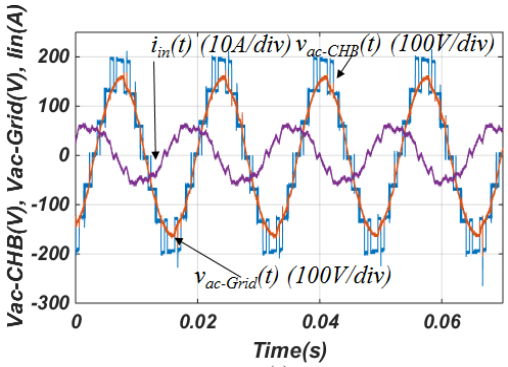

(a)

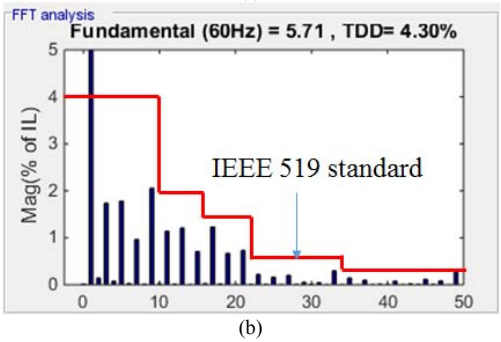

(b)

Fig. 7, Waveforms of the CHB converter in steady state condition, (a) time-domain waveforms of the $v_{ac\text{-}CHB}(t)$, $v_{ac\text{-}Grid}(t)$, and $i_{in}(t)$, (b) harmonic spectrum of the $i_{in}(t)$.

In the second experimental results, the discharging current of the CHB converter with one percent SOC difference between the SOCs of cells are shown. Fig. 8 shows the SOCs of the two conventional techniques [10-11] and the two proposed techniques when the AC current is controlled to 4.2A and 120 degrees. As shown in Fig. 8(a), the first conventional technique [10] cannot balance the SOCs of the CHB converter within 500s. The second conventional technique [11] can only balance the SOCs of the second and third cells of the converter within 500s. However, the first cell does not balance the SOC within 500s. In Fig. 8 (c), all of the three cells of the CHB converter are balanced around 440s for the first proposed technique due to applying optimized switching transitions to the CHB converter by checking the instantaneous active power. In Fig. 8 (d), the experimental results of the second proposed technique are shown. It is obvious that by checking the sign of AC input current to balance the SOCs instead of the instantaneous active power, the SOCs can be balanced much faster. So, the second proposed technique can balance the SOCs within 400s which is 40s faster than the first proposed technique.

In Fig. 9, the average currents of the cells of the CHB converter are shown. As shown in Fig. 9, the first conventional, the first proposed and the second proposed techniques have almost constant average currents before SOCs are balanced. However, the second conventional technique has huge AC ripple due to asymmetric switching states of different cells of the CHB converter.

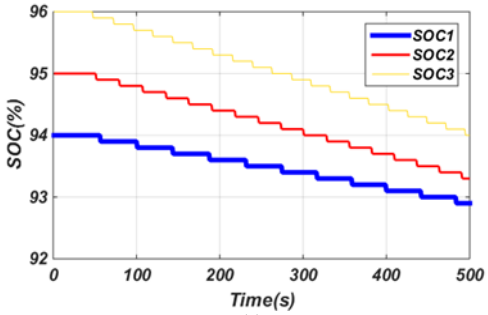

(a)

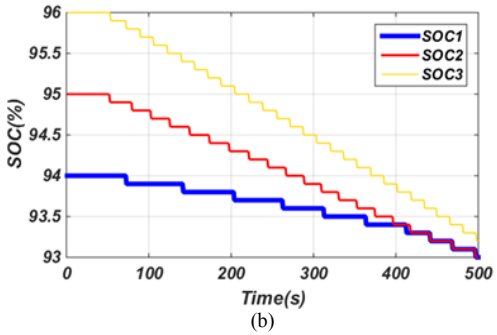

(b)

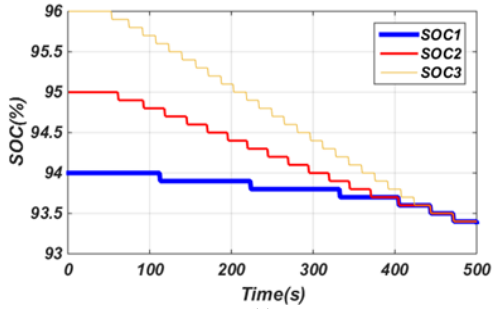

(c)

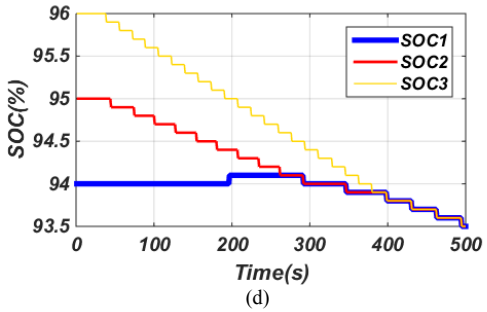

(d)

Fig. 8, SOCs of the four SOC balancing techniques during discharging condition. (a) The first conventional technique [10], (b) The second conventional technique [11], (c) The first proposed technique, (d) The second proposed technique.

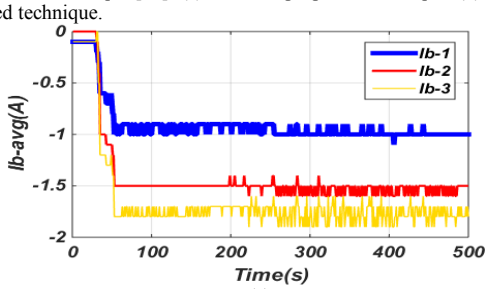

(a)

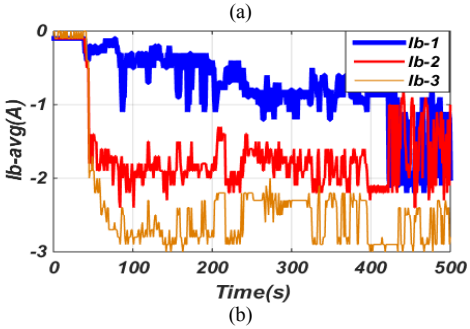

(b)

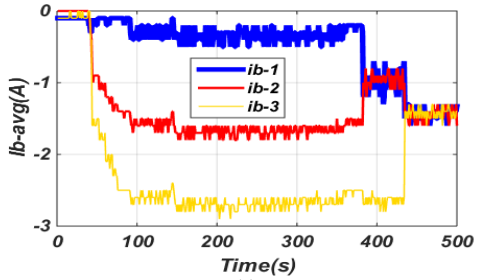

(c)

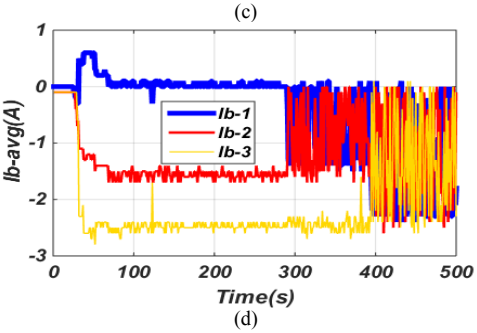

(d)

Fig. 9, $I_{b\text{-}avg}$ of the four SOC balancing techniques during discharging condition. (a) The first conventional technique [10], (b) The second conventional technique [11], (c) The first proposed technique. (d) The second proposed technique.

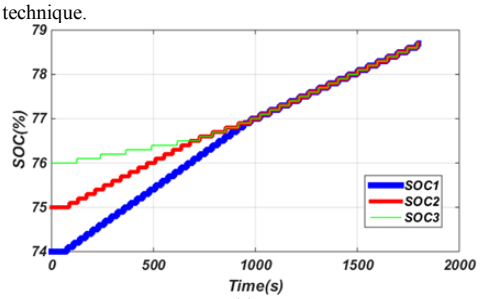

(a)

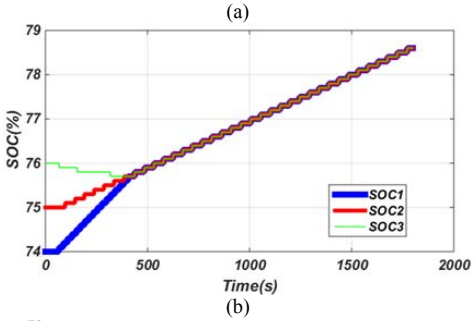

(b)

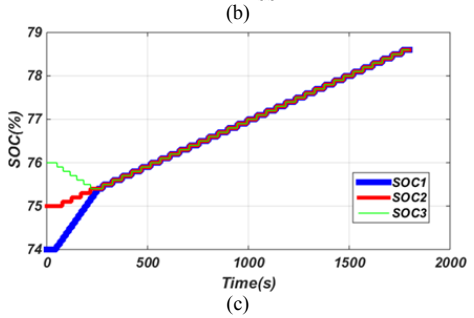

(c)

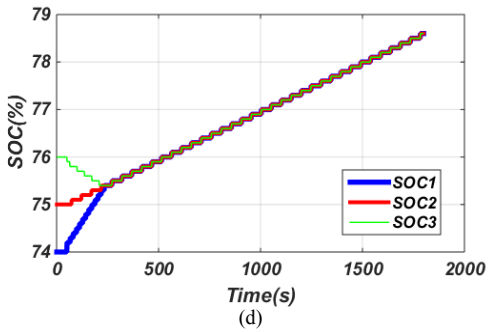

(d)

Fig. 10, SOCs of the four SOC balancing techniques during charging condition. (a) The first conventional technique [10], (b) The second conventional technique [11], (c) The first proposed technique. (d) The second proposed technique.

In the last experiment in Fig. 10, the charging process of these four techniques are compared. As shown in Fig. 10 (a), when the AC input current of the CHB converter is controlled to 6.4A and 70 degrees, the four techniques can balance the SOCs of the CHB converter with different balancing speeds. From Fig. 10 (a), it is obvious that the SOCs of cells can be balanced in less than 900s when the SOCs have one percent difference between the SOCs of cells at the beginning of charging for the first conventional technique [10]. However, the second conventional technique requires around 400s to balance the three SOCs of cells. This higher speed of balancing the SOCs is achieved with unequal power losses on different switches of the CHB converter which is undesirable. To obtain the optimized charging performance, the two proposed techniques in this paper can balance the SOCs of the CHB cells in less than 250s as shown in Fig. 10 (c) and (d). In Fig. 10 (c), the charging performance of the first proposed technique is shown. It can be observed that the first proposed technique can balance the SOCs in less than 250s. Also, the second proposed technique can balance the SOCs in 240s as shown in Fig. 10(d). Even though the second proposed technique shows improvement in charging, it is possible to increase the balancing speed of SOC by optimally selecting the switching states of the CHB based on the obtained switching angles of SHCM-PWM for different modulation indices and different phase of the AC current.

V. Conclusions

In this paper, two new SOC balancing techniques were proposed for the CHB multilevel converter. The first proposed technique uses the redundant states and the instantaneous active power that is injected to the CHB converter to balance the SOCs of cells of the CHB converter. The second proposed technique uses the sign of AC input current of the CHB and the switching angles of modulation technique to balance the SOCs of the CHB converter. As shown in the experimental results, the two proposed techniques can balance the SOCs of batteries much faster than two conventional techniques when the power losses of switches in each cell are equally distributed.

References

[1] M. Liu, W. Li, C. Wang, M. P. Polis, L. Y. Wang and J. Li, "Reliability Evaluation of Large Scale Battery Energy Storage Systems," in *IEEE Transactions on Smart Grid*, vol. 8, no. 6, pp. 2733-2743, Nov. 2017.

[2] Khazaei, P., S. M. Modares, M. Dabbaghjamanesh, M. Almousa, and A. Moeini. "A high efficiency DC/DC boost converter for photovoltaic applications." *International Journal of Soft Computing and Engineering (IJSCE)* 6, no. 2 (2016): 2231-2307.

[3] S. Wang, R. Crosier and Y. Chu, "Investigating the power architectures and circuit topologies for megawatt superfast electric vehicle charging stations with enhanced grid support functionality," *Electric Vehicle Conference (IEVC), IEEE International*, Greenville, SC, 2012, pp. 1-8.

[4] A. Moeini, Z. Hui, and S. Wang, "Improve Control to Output Dynamic Response and Extend Modulation Index Range with Hybrid Selective Harmonic Current Mitigation-PWM and Phase-shift PWM for Four-Quadrant Cascaded H-Bridge Converters" *IEEE Transactions on Industrial Electronics*, 2017.

[5] A. Moeini, H. Zhao, and S. Wang "A Current Reference based Selective Harmonic Current Mitigation PWM Technique for Cascaded H-bridge Multilevel Active Rectifiers with Small Coupling Inductance, Extended Harmonic Reduction Spectrum and the Ability to Reduce the Harmonic Currents due to Grid Voltage Harmonics" *IEEE Transaction on Industrial Electronics*, 2017.

[6] Dabbaghjamanesh, M., A. Moeini, M. Ashkaboosi, P. Khazaei, and K. Mirzapalangi. "High performance control of grid connected cascaded H-Bridge active rectifier based on type II-fuzzy logic controller with low frequency modulation technique." *International Journal of Electrical and Computer Engineering* 6, no. 2 (2016): 484.

[7] M. Aleenejad, H. Mahmoudi and R. Ahmadi, "Unbalanced Space Vector Modulation with Fundamental Phase Shift Compensation for Faulty Multilevel Converters," in *IEEE Transactions on Power Electronics*, vol. 31, no. 10, pp. 7224-7233, Oct. 2016.

[8] Marzoughi, Alinaghi, Hossein Imaneini, and Amirhossein Moeini. "An optimal selective harmonic mitigation technique for high power converters." *International Journal of Electrical Power & Energy Systems* 49 (2013): 34-39.

[9] A. Moeini and S. Wang, "A DC Link Voltage Balancing Technique for Cascaded H-Bridge Multilevel Converters with Asymmetric Selective Harmonic Current Mitigation-PWM," in *IEEE Transactions on Power Electronics*, 2017.

[10] Young, Chung-Ming, Neng-Yi Chu, Liang-Rui Chen, Yu-Chih Hsiao, and Chia-Zer Li. "A single-phase multilevel inverter with battery balancing." IEEE Transactions on Industrial Electronics 60, no. 5 (2013): 1972-1978.

[11] Gholizad, Amin, and Murtaza Farsadi. "A Novel State-of-Charge Balancing Method Using Improved Staircase Modulation of Multilevel Inverters." IEEE Transactions on Industrial Electronics 63, no. 10 (2016): 6107-6114.

[12] Moeini, Amirhossein, Hossein Iman-Eini, and Alinaghi Marzoughi. "DC link voltage balancing approach for cascaded H-bridge active rectifier based on selective harmonic elimination-pulse width modulation." *IET Power Electronics* 8, no. 4 (2015): 583-590.

[13] IEEE Recommended Practice and Requirements for Harmonic Control in Electric Power Systems," in IEEE Std 519-2014 (Revision of IEEE Std 519-1992), vol., no., pp.1-29, June 11 2014.

[14] Ashkaboosi, Maryam, Seyed Mehdi Nourani, Peyman Khazaei, Morteza Dabbaghjamanesh, and Amirhossein Moeini. "An optimization technique based on profit of investment and market clearing in wind power systems." *American Journal of Electrical and Electronic Engineering* 4, no. 3 (2016): 85-91.

[15] M. Dabbaghjamanesh, S. Mehraeen, A. Kavousifard and M. A. Igder, "Effective scheduling operation of coordinated and uncoordinated wind-hydro and pumped-storage in generation units with modified JAYA algorithm," 2017 IEEE Industry Applications Society Annual Meeting, Cincinnati, OH, USA, 2017, pp. 1-8.

[16] A. Moeini and S. Wang, "A DC Link Voltage Balancing Technique for Cascaded H-Bridge Multilevel Converters with Asymmetric Selective Harmonic Current Mitigation-PWM," in *IEEE Trans. on Power Electron*, (early access).